European Journal of Agronomy 86 (2017) 60–70

Contents lists available at ScienceDirect

European Journal of Agronomy

journal homepage: www.elsevier.com/locate/eja

Cytokinins: A key player in determining differences in patterns of canopy senescence in Stay-Green and Fast Dry-Down sunflower (*Helianthus annuus* L.) hybrids

Mariano A. Mangieri*, Antonio J. Hall, Gustavo G. Striker, Claudio A. Chimenti

IFEVA, Universidad de Buenos Aires/CONICET, Facultad de Agronomía, Buenos Aires, Av. San Martín 4453, C1417DSE, Argentina

ARTICLE INFO

Keywords:
Sunflower
Root functionality
Cytokinins
Threshold of cytokinin
Leaf senescence
Canopy senescence

ABSTRACT

Leaf senescence during grain filling can reduce crop yield. We studied, under field conditions and during grain-filling, the association between leaf cytokinin levels and the onset of leaf senescence in sunflower hybrids of contrasting canopy senescence patterns (Paraiso75, stay-green [SG] and Paraiso65, fast dry down [FDD]). At crop level, dynamics of live root length density (LRLD) and green leaf area index (GLAI) were followed, while at leaf level dynamics of total chlorophyll content, *trans*-Zeatin content, net photosynthesis and PSII quantum yield, were followed in leaf positions 17, 20, 22 and 24. Responses of these leaf variables to exogenous cytokinin applications to leaves at position 17 were also followed. SG exhibited greater ($p < 0.05$) LRLD and GLAI values at anthesis. In both hybrids, LRLD began to fall before GLAI. All variables decreased earlier ($p < 0.05$) in FDD. Initial leaf levels of *trans*-Zeatin were three times higher ($p < 0.05$) in SG. Exogenous cytokinin applications maintained leaf-level variables. These are the first results showing associations between LRLD dynamics with the dynamics of leaf cytokinin levels and changes in indicators of leaf functionality. Also, this is the first study in which estimates are made of cytokinin thresholds below which leaf senescence begins in two hybrids of contrasting canopy senescence patterns. These advances in the understanding, at both crop and leaf levels, of the controls and consequences of SG during grain filling, a trait known to improve crop water uptake under drought and increase biomass accumulation during grain filling, provide support for breeding efforts aimed at profiting from this trait to increase crop yields.

1. Introduction

Accelerated leaf senescence during grain filling can significantly reduce crop yield due to reductions in the levels of photoassimilate available for grain filling, as documented in barley (*Hordeum vulgare* L.) and wheat (*Triticum aestivum* L.) (Gregersen et al., 2008) and in maize (*Zea mays* L.) (Rajcan et al., 1999; Rajcan and Tollenaar, 1999). During leaf senescence the rupture of chloroplasts (Guiamét et al., 1999), the catabolism of chlorophyll and macromolecules, such as proteins (Lamattina et al., 1985; Martínez et al., 2008), nucleic acids and membrane lipids takes place, in what is referred to as the decommissioning process of the photosynthetic apparatus. This results in the re-mobilization of much of the N content of photosynthetic proteins to other growing organs (Lim et al., 2007).

In monocarpic species, leaf senescence is coordinated with senescence of whole plant and influenced by endogenous and exogenous factors. The regulation of this physiological process does not follow a simple signal transduction chain, but is influenced by a network of internal and external signals (He et al., 2001; Gan and Amasino, 1997; Buchanan-Wollaston et al., 2003 Gan and Amasino, 1997; Buchanan-Wollaston et al., 2003). Among the external signals, stress factors such as drought (Pic et al., 2002) and changes in the quality and intensity of light (Guiamét et al., 1989; Rousseaux et al., 1996, 2000) can play a part. Among the internal signals phytohormones (Noodén et al., 1997), root functionality (Lisanti et al., 2013) and demand for nitrogen by non-leaf organs, especially grain (Sinclair and De Wit, 1976; Sinclair and Horie, 1989; Van Oosterom et al., 2010) can have important roles in the induction of senescence. Among the hormones involved, cytokinins delay the process (Lim et al., 2007).

The predominant cytokinins in higher plants are isopentenyladenine, zeatin and dihydrozeatin (Sakakibara, 2006). Usually zeatin is the most abundant natural free cytokinin. Zeatin in higher plants is present in trans and cis forms, and these can be interconverted by zeatin isomerase. The *trans*-Zeatin form is more active in biological assays. The primary sites of synthesis of free cytokinins in whole plants are the apical meristems of roots (Akiyoshi et al., 1983; Akiyoshi et al., 1984;

* Corresponding author.
E-mail address: mangieri@agro.uba.ar (M.A. Mangieri).

http://dx.doi.org/10.1016/j.eja.2017.03.007
Received 13 September 2016; Received in revised form 23 March 2017; Accepted 31 March 2017

Barry et al., 1984; Beveridge et al., 1997; Samuelson et al., 1992; Takei et al., 2001; White, 1934). Cytokinins synthesized in roots move through the xylem together with water and minerals absorbed by the roots (Itai and Vaadia, 1971; Takei et al., 2001). In xylem exudate, cytokinins are mainly found in the form of zeatin riboside (Takei et al., 2001). Noodén et al. (1990) found, in the xylem exudate of soybean (*Glicine max* L.), that zeatin riboside, dihydrozeatin riboside, zeatin and dihydrozeatin were the most important forms of cytokinins present in the exudate, although further possible unknown forms could not be ruled out.

Gan and Amasino (1995), in tobacco (*Nicotiana tabacum* L.), found that the cytokinin content in senescent leaves decreases, and this has been proposed as a key signal involved in canopy senescence. The reduction of the cytokinin flow from the roots apparently fulfills an important role in soybean canopy senescence, and this reduction seems to be induced by messages from pods (Noodén et al., 1990). In maize (Ren et al., 2016), rice (*Oryza sativa* L.) (Liu et al., 2016), and tobacco (Singh et al., 1992) it has been shown that the application of cytokinins to leaves delays their senescence.

In many annual crops it has been observed that root biomass values reach a maximum at around flowering (Gregory et al., 1978; wheat; Mengel and Barber, 1974; maize; Sadras et al., 1989; sunflower). From this point onwards, root biomass begins to decline or, in some cases remains constant, and the same occurs with the functionality of the root system. Lisanti et al. (2013) found, in sunflower, a significant decrease of root biomass and of live root length density after flowering, effects that were associated with reductions in the volume of water absorbed by the crop. They also found that during the grain filling phase live root length density began to decrease before leaf senescence became evident. This phase is critical to crop performance because during it grain weight per plant is determined, therefore water and nutrient supply, especially of nitrogen, is of great importance for crop yield.

In sunflower variability exists in the patterns of canopy senescence during grain filling, ranging between the extremes of delayed senescence (stay-green, SG) and rapid senescence (fast dry down, FDD), and these differences are linked to variations in the accumulation of post-anthesis biomass (De la Vega et al., 2011). Furthermore, Lisanti et al. (2013) found, under both drought and irrigation, that a SG sunflower hybrid maintained greater soil water extraction rates for a longer time after flowering than a FDD hybrid, in association with a greater live root length density. This set of observations suggests that sunflower, in its SG and FDD forms, is an appropriate experimental model to examine the possible role of cytokinins in the control of leaf senescence and their role in the root/leaf communication during the grain filling phase.

The objectives of the present study were: 1) to track, in sunflower hybrids of contrasting canopy senescence patterns (SG and FDD), the dynamics of cytokinin levels in leaves during grain filling, and their association with root functionality and leaf senescence. Leaf cytokinin levels in the leaves were also manipulated by exogenous application of cytokinins to the leaves, something which aimed to 2) establish the threshold cytokinin level below which leaf senescence is triggered. In relation to the first objective, we postulated two hypotheses. The first that both timing of the onset and the rate of leaf senescence are strongly associated with levels of cytokinins in the leaves; variables which, in turn, would be linked to the observed differences in the dynamics of leaf senescence between SG and FDD hybrids. The second was that the cytokinin levels in the leaves are associated with the level of root functionality during grain filling. In consequence, the SG hybrid was expected to exhibit a more extended period of root functionality and maintain leaf cytokinin levels for longer periods than the FDD hybrid. In relation to the second objective, our hypothesis was that exogenous cytokinin applications would increase the level of this phytohormone in the leaves, reversing or delaying the onset of leaf senescence. There is no precedent in the literature, for sunflower or any other crop species, of studies that sought to document, in a simultaneous fashion, these variables in cultivars with different patterns of canopy senescence. Moreover, there are no precedents in sunflower, or in any other crop species, of attempts to determine the cytokinin levels below which the process of leaf senescence is triggered.

2. Materials and methods

2.1. Experimental design and crop growth conditions

The experiments were carried out at the Faculty of Agronomy, University of Buenos Aires (34° 35′S, 58° 29′W) during two growing seasons (2012/13 and 2013/14). Sowing dates were 22/11/12 and 30/11/13. Two sunflower hybrids (Nidera Semillas SA, Argentina), which do not differ in length of cycle or time to flowering but exhibit different canopy senescence patterns between flowering and physiological maturity, were used. Paraiso 75 belongs to the “SG” type and has greater green leaf area duration, while Paraiso 65 belongs to the “FDD” type and exhibits a greater canopy senescence rate during post-anthesis. The crops were grown under field conditions at a density of 7.5 plants m^{-2} (achieved by over-planting and thinning at 4-true-leaf stage), fertilized and protected from insects and diseases. The whole of the experimental area was protected from rain with a moveable rain-out shelter for the entire season, in order to avoid proliferation of foliar diseases. A split-plot experimental design with five replicates was used. Each of the five main plots contained two subplots, one for each hybrid (SG and FDD). Each main plot size contained 14 (seven for each sub-plot) 4.5 m-rows, spaced at 0.65 m between rows and each plot was fitted with an independent drip-irrigation system. The amount of water supplied differed between irrigations according to atmospheric demand, and aimed at maintaining soil water status close to field capacity.

Crop developmental status was recorded at weekly intervals using the Schneiter and Miller (1981) scale from the stage of twelve true leaves (V12) through to physiological maturity (R9, inflorescence bracts become yellow and brown). Three non-contiguous representative plants, in perfect competition and away from sub-plot borders and row extremes, were tagged in each sub-plot and used to record crop phenology.

During the grain filling period average daily incident PAR and average daily temperature were recorded using a 21X data-logger (Campbell Scientific Inc., Logan, UT), fitted with an HMP35C (Campbell Scientific, Inc) temperature sensor, and Li190SB PAR sensor (Li-Cor, Lincoln, NE) located at 40 m from the center of the experiment.

2.2. Response variable measurements

2.2.1. Live root length density (LRLD)

Every 7 or 8 days, commencing 8 days before the beginning of anthesis (Stage R5.1, 10% of the head area [disk flowers] in anthesis) and through to physiological maturity (Stage R9), samples were taken from the 0–20, 20–40 and 40–60 cm soil layers (more than 90% of the root system in sunflower is located in the 0–60 cm soil layer (Sadras et al., 1989; Angadi and Entz, 2002)) of each sub-plot. To do this a 5-cm diameter aluminum tube was inserted perpendicular to the soil surface at the midpoint between two representative neighboring plants in a row that were in perfect competition and away from sub-plot borders and row extremes. Three samples per position were taken in each of the five sub-plots. At each sampling position the tube was inserted three times in sequence to the required depths, and the resulting cylinders of soil released using a piston of a diameter equal to that of the internal one of the tube. Immediately after extracting each cylindrical sample, a 1.5-cm diameter soil core sampler was used to subsample that cylinder at three positions (one at each of the extremes and one at the cylinder mid-point, each aligned with the diameter of the sample core). Roots present in these three sub-samples were washed free of soil on a 590 μm mesh sieve and combined to form the composite sample using the Lisanti et al. (2013) technique, and this composite sample was used to

determine live root length density using the Sturite et al. (2005) technique. Roots in the composite sample were infiltrated under vacuum (20 min at 0.3 bar suction) with a solution prepared with 50 ml 0.6% (w/v) 2, 3, 5-triphenyl tetrazolium chloride (TTC), 50 ml of 0.06 M phosphate buffer and 50 ml 0.05% (v/v) of a wetting agent (Tween 20). After infiltration roots were incubated at 30 °C for 20 h in the same solution. At the end of this treatment protocol, live roots are red. After incubation, roots were evenly distributed on the surface of a square dish and scanned using an EPSON Expression1600 scanner (Seiko EPSON Corp, Japan) with a resolution of 400 dpi. The scanned images were analyzed using a Winrhizo version Pro V 2008 (Regent Instruments Inc, Canada) analyzer system to determine living and dead root numbers and length as a function of colour discrimination. Live root length density was estimated as live root length per unit sample volume.

2.2.2. Green leaf area index (GLAI)

From the appearance of leaf 12 (V12) and until all the leaves had reached full expansion, individual leaf dimensions (length, width) were measured at weekly intervals on three previously tagged randomly distributed and non-contiguous representative plants from the central portion of each sub-plot of the five plots, and individual leaf areas were estimated as the product of width and length multiplied by 0.75 (Pereyra et al., 1982). Plant leaf area was estimated as the sum of these values and used to estimate crop GLAI. Measurements were performed as from the appearance of leaf 12, since the leaves above this position are those most associated with leaf senescence during the grain filling phase (Dosio et al., 2010). Once leaf senescence began, we recorded the proportion of each individual leaf that had turned yellow and discounted the senescent area per plant (and that of abscised leaves) from plant green leaf area.

2.2.3. Leaf variables

2.2.3.1. Total chlorophyll. To determine the onset of senescence, measurements of total chlorophyll content were performed daily using a portable chlorophyll meter (SPAD 502, KonicaMinolta, NJ), starting at mid-anthesis (Stage R5.5, 50% of the head area [disk flowers] in anthesis), on targeted leaves of three randomly distributed non-contiguous representative tagged plants from the central portion of each sub-plot of the five plots. These measurements continued until 50% of the area of the targeted leaf turned yellow. A linear function fitted to the total chlorophyll/SPAD relationship ($0.084x - 0.463$, $R2 = 0.9$, $n = 75$), was used to estimate total chlorophyll values, of the both hybrids, on the basis of SPAD readings. To calibrate this function, we selected leaves of both hybrids which covered the visual range from green to yellow and a SPAD range from 1.9 to 50.9. Three 5-mm diameter discs were extracted from each leaf with a punch, a SPAD measurement performed on those discs and the resultant values averaged. Discs were then dried with tissue paper and weighed to determine their fresh weight. The 3 discs were placed in a candy-colored flask containing 3 ml of N, N-dimethylformamide and left in the dark for twelve hours. The absorbance of the resulting solution was measured, after vigorous shaking of the flasks, at wavelengths of 664 nm (chlorophyll A) and 647 nm (chlorophyll B) using a spectrophotometer (UV-1700 series, Shimadzu, Kyoto, Japan). Absorbance values at both peaks were entered into the total chlorophyll equation in N, N-dimethylformamide solution proposed by Inskeep and Bloom (1985) and were corrected by the solvent volume used and the fresh weight of the discs. The targeted leaves were those at positions 17, 20, 22 and 24 (acropetal sense). At the start of SPAD measurements, leaf 17 was two positions above the uppermost leaf showing signs of yellowing. Eight SPAD measurements per leaf, separated from each other by 3 cm and distributed from the apex to the base of the lamina, were performed for each individual leaf (Guiboileau et al., 2010). Onset of senescence of a targeted leaf was assumed to occur when total chlorophyll levels began to decrease, as reflected in the daily SPAD measurements, and later corroborated by fitting bilinear regressions to the data.

2.2.3.2. Net photosynthesis and maximum quantum yield of PSII. Measurements of leaf net photosynthesis and maximum quantum yield of PSII *(Fv/Fm)* were performed daily, starting at mid-anthesis (Stage R5.5) and continuing until 50% of the area of the targeted leaves were senescent, on leaves of three randomly distributed non-contiguous tagged plants from the central portion of each sub-plot of the five plots. Net photosynthesis at a photosynthetic photon flux density (PPFD) of 1500 μmol m^{-2} s^{-1} was measured using a Li-6400 portable photosynthesis system (Li-Cor Inc., Lincoln, Nebraska, USA). Light was provided by the 6400-40 leaf chamber light source using a mix of 80% red and 20% blue light. Air flow, CO_2 concentration in the chamber and block temperature were controlled automatically by the equipment at 300 μmol s^{-1}, 400 μmol mol^{-1} (ppm) and 27 °C, respectively.

Maximum quantum yield of PSII *(Fv/Fm)* was measured on the same target leaves using a FMS 2 chlorophyll fluorometer (Hansatech Instruments, Pentney, King's Lynn, Norfolk, United Kingdom).

2.2.3.3. Leaf trans-Zeatin contents. To quantify leaf cytokinin levels, samples were taken starting at mid-anthesis (Stage R5.5), prior to, during and after onset of senescence, from leaves located at positions 17, 20, 22 and 24 of one representative tagged plant from the central portion of each sub-plot of the five plots. Before starting measurements, randomly distributed plants in the same development stage were selected. The samples were taken from different plants on each occasion because measurements were destructive. Prior to the onset of leaf senescence samples were taken every three days. Once senescence (see Section 2.2.3.1.) started in a particular leaf position, that position was sampled every two days until 50% of the area of that leaf was senescent. Samples were frozen in liquid N2 for 24 h, and then kept at −20 °C until chemical analysis. Extraction, purification and quantification of cytokinins from samples were performed as described by Hoyerová et al. (2006). We elected to measure *trans*-Zeatin levels in leaves in the light of the evidence that it is one of the dominant cytokinin involved in the control of leaf senescence and because changes in levels of other cytokinins tend to occur in parallel with those of Zeatin (Noodén et al., 1990). Determinations of *trans*-Zeatin levels in leaves were performed by high pressure liquid chromatography (HPLC) using an Agilent 1100 series (Agilent, Germany) chromatograph, and zeatin quantified using an internal *trans*-Zeatin standard (trans-Zeatin, Sigma Aldrich Argentina).

2.2.3.4. Exogenous cytokinin applications. Three exogenous applications of two different types of cytokinin were made on position 17 (acropetal sense) leaves on five, per type of cytokinin, representative tagged plants from the central portion of each sub-plot of the five plots. Applications were performed on position 17 leaves, because this leaf was located two positions above the one that presented visual signs of senescence in mid-anthesis (Stage R5.5). The first of these applications were made at the onset of senescence of this leaf (as reflected in SPAD values, see Section 2.2.3). After application, we monitored leaf total chlorophyll values until they decreased again, at which stage the second application was performed. Monitoring of total chlorophyll content was then repeated, and when values of this variable fell once again, the third application was performed. In addition we monitored leaf net photosynthesis and maximum quantum yield of PSII (*Fv/Fm*) throughout the treatment period. The application volume was 2.3 ml per leaf of a solution containing 8 ppm of 6- benzylaminopurine (BAP, synthetic) or zeatin (Z, natural) (application volume and cytokinin concentrations were selected on the basis of the results of preliminary experiments using a range of concentrations and volumes). The following 6 treatments were defined: 1) SG Control; 2) SG BAP 8 ppm; 3) SG *trans*-Zeatin 8 ppm; 4) FDD Control; 5) FDD BAP 8 ppm;

6) FDD *trans*-Zeatin 8 ppm. Leaves were sampled before and after the application of exogenous cytokinin. The samples were stored and analyzed for determining endogenous *trans*-Zeatin levels as described in the Materials and methods section, Response variable measurements, Leaf variables, Leaf *trans*-Zeatin contents.

2.2.4. Intensity and quality of light incident on target leaves

In order to exclude the possibility that differences in light intensity or quality (Rousseaux et al., 1996, 2000; Guiamét et al., 1989) were involved in determining the differences in the timing of onset of senescence in leaves 17, 20, 22 and 24 of the FDD and SG hybrids, we measured the intensity and quality of the light incident on those leaves at the beginning of R5 (1 day from the beginning of anthesis [DFBA]), R6 (12 DFBA), R7 (22 DFBA) and R8 (30 DFBA) on leaf positions of three randomly distributed non-contiguous representative tagged plants from the central portion of each sub-plot of the five plots. Both measurements were performed between 11:00 and 14:00 h. Radiation was measured using a PAR quantum sensor (Li-Cor Q 24122) attached to a LI-1000 (Li-Cor Inc., Lincoln, Nebraska, USA) portable meter, and the red/far-red ratio (R/FR) using a portable Red/Far-Red (660/730) meter (SKR 100 36100, Skye Instruments Llandrindod Wells, Powys, United Kingdom).

2.3. Statistical analyses

For most of the response variables (LRLD, GLAI, Total Clorophyll, Net photosynthesis, Fluorescence and *trans*-Zeatin leaf contents), segmented linear regressions (also called bi-linear regressions) were fitted using Graph Pad Prism software (version 5.00 for Windows, Graph Pad Software, San Diego, CA, USA, http://www.graphpad.com/). Bi-linear functions were preferred to polynomials, because they allow for simpler comparisons between treatments, and because visual inspection of the dynamics of these variables indicated that this approach provided appropriate descriptions of the data. To determine the significance of differences between treatments across the 2 years of experiments we compared the values of the parameters of the functions fitted to the various response variable/time relationships (i.e., the y-axis intercept, the slope of initial segment, the value of the independent variable corresponding to the break point between the two segments, and the slope of the second linear segment) using analysis of variance (ANOVA) as implemented in the Infostat/Professional V.2011 software (Di Rienzo et al., 2010). The Tukey test was used to define the significance of differences between treatments. An equivalent approach was used to contrast the values of PAR and of R/FR of light incident on each leaf position across hybrids for each sampling time and year.

3. Results

3.1. Year- treatment interactions

No significant ($p > 0.05$) hybrid by year interactions were found for the coefficients of the bi-linear functions fitted to the dynamics of LRLD, GLAI, Total Clorophyll, Net photosynthesis, Fluorescence and *trans*-Zeatin leaf content (Tables S1–S3 Supplementary material). The response patterns of leaf variables evoked by the application of exogenous cytokinins were very similar, within each hybrid, in both years (data not shown). No significant ($p > 0.05$) hybrid by year interactions were found for PAR and R/FR levels of light incident on leaves at each position at each sampling date (Table S4).

The FDD hybrid reached Stage 5.1 (beginning of anthesis) at 1153 °Cd and 1156 °Cd [T_b = 4 °C, Villalobos and Ritchie (1992)] after sowing, in Years 1 and 2 respectively; while the SG hybrid reached the same stage at 1195 °Cd and 1205 °Cd, in Years 1 and 2 respectively. Physiological maturity (Stage R9) was reached at 46 DFBA in both hybrids in both years. During the period between R5.1 and R9, and for the FDD hybrid, the average daily air temperature (°C) was 24.7 °C and 24.8 °C in Years 1 and 2 respectively; while for the SG hybrid the corresponding values were 24.4 °C and 24.5 °C. The average daily incident PAR for the FDD hybrid during the period between R5.1 and R9 were 33.1 and 32.8 mol m^{-2} d^{-1} in Years 1 and 2 respectively; and the equivalent values for the SG hybrid were 33.2 and 32.6 mol m^{-2} d^{-1}. Thus, the environmental conditions during the measurement period were similar among hybrids within years and between years within each hybrid.

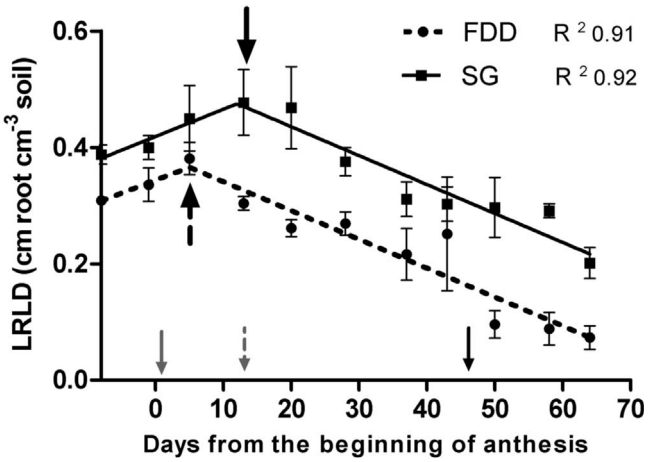

Fig. 1. Dynamics, during grain filling, of live root length density (LRLD) in the 0–60 cm soil layer for SG and FDD hybrids. Broad full and dashed vertical arrows indicate the timings of achievement of peak LRLD values of SG and FDD hybrids, respectively. The arrows close to "x" axis indicate the timings of R5.1 (narrow full gray arrow), R6 (narrow dashed gray arrow) and R9 (narrow full black arrow). Capped vertical bars on data points indicate ± 1 S.E. (n = 5). R^2 values for the fitted functions are shown next to treatment codes. For parameter values of fitted functions, see Table S3, Supplementary material. Data from Year 1.

Based on these general similarities between years of the response patterns of the measured variables within each hybrid, the crop development rates in each of the SG and FDD hybrids, and the similarity in environmental conditions during grain filling across years and hybrids, in what follows and in the interests of simplicity, data from a single year only is presented to illustrate responses.

3.2. Live root length density (LRLD)

The samples from the 0–20 cm, 20–40 cm and 40–60 cm soil layers showed similar time trends, so data for all layers were pooled and the pooled values for the 0–60 cm layer are shown (Fig. 1). The significant ($p < 0.05$) delay in the timing of the change in slope of LRLD variation from positive to negative of SG with respect to FDD was 7 days (Table S3, Supplementary material). In addition, peak values for LRLD were significantly ($p < 0.05$) greater (26.3%) in SG than FDD. From the time of achievement of peak LRLD values until R9, rates of decrease in LRLD were statistically indistinguishable ($p > 0.05$) between hybrids. Importantly, this pattern meant that the SG hybrid exhibited greater LRLD values throughout the grain-filling phase, and the difference between hybrids became proportionally greater as the grain-filling phase advanced (Fig. 1). Thus, at 50 DFBA (a few days after R9) values for LRLD were significantly ($p < 0.05$) greater (200%) in SG than FDD.

3.3. Green leaf area index (GLAI)

The timing of the change in the rate of GLAI variation from plateau to negative were significantly ($p < 0.05$) later in SG (18 DFBA) with respect to FDD (12 DFBA) (Fig. 2). In addition, the maximum values of GLAI were significantly ($p < 0.05$) greater in SG than FDD in both years. From the time of the start of the fall in GLAI values and until R9, rates of decrease in GLAI were statistically indistinguishable ($p > 0.05$) between hybrids in both years (Table S3, Supplementary

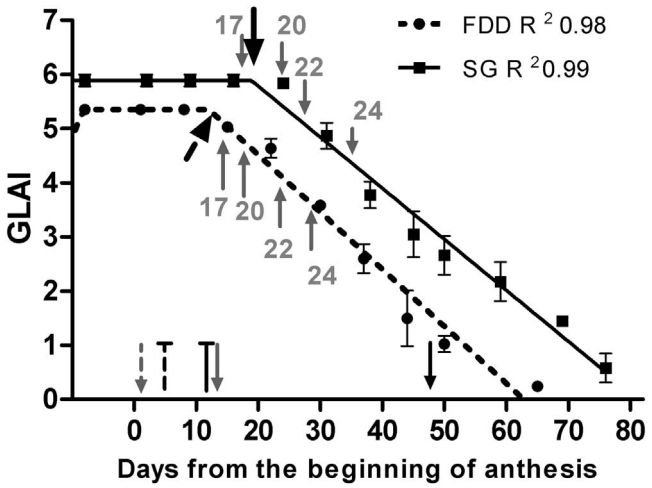

Fig. 2. Dynamics, during grain filling, of green leaf area index (GLAI) for SG and FDD hybrids. The onset time of the fall in GLAI is indicated with full (SG) or dashed (FDD) broad black arrows. The arrows close to "x" axis indicate the timings of R5.1 (narrow full gray arrow), R6 (narrow dashed gray arrow), and R9 (narrow full black arrow). Capped vertical lines close to the "x" axis indicate the start of the falls in LRLD (dashed, FDD; full, SG). Narrow full gray arrows close to the GLAI/time functions for each hybrid indicate the onset of the senescence of designated leaf positions. Capped vertical bars on data points indicate ± 1 S.E. (n = 5). R^2 values for the fitted functions are shown next to treatment codes. For parameter values of fitted functions, see Table S3, Supplementary material. Data from Year 1.

material). Importantly, because the SG hybrid maintained the maximum values in GLAI for several days after this variable started to decrease in the FDD hybrid, the former exhibited greater GLAI values throughout the grain filling phase, and this difference became proportionally greater as the grain-filling phase advanced (Fig. 2). Thus, at 50 DFBA (a few days after R9) values for GLAI were significantly ($p < 0.05$) greater (87% in Year 1, 76% in Year 2) in SG than FDD in both years.

3.4. Leaf total chlorophyll dynamics

The dynamics of total chlorophyll in all four targeted leaf positions and the differences in these dynamics between hybrids and leaf positions are exemplified for Year 1 in Fig. 3. The basic dynamic consisted of a plateau value that persisted over time until a break point, after which the chlorophyll level dropped linearly. The interactions between hybrids and leaf positions were significant ($p < 0.05$) for both the timing of the start of the fall and for the rate of fall of chlorophyll levels (both in units of thermal time [Tb = 4 °C] from achievement of maximum leaf size) (Table S2, Supplementary material). These interactions were mostly attributable to the dynamics of chlorophyll level in Leaf 17, in which slight differences between hybrids in the falling phase rate resulted in similar chlorophyll values in both hybrids as from 600 °Cd from maximum expansion of this leaf. The maximum values of total chlorophyll were statistically indistinguishable ($p > 0.05$) between hybrids and leaf positions. The broad picture arising from the data of Fig. 3 is that the start of the falling phase was later ($p < 0.05$) in all four leaf positions in SG, resulting –for Leaves 20, 22 and 24- in greater chlorophyll levels in SG during the whole of the falling phase. Virtually no significant differences ($p > 0.05$) were found between positions in each hybrid in the start of falling phases. Small, although sometimes significant, differences in the falling phase slopes (Tables S2 and S3, Supplementary material and Fig. 3) did not alter this general panorama. The differences between hybrids in the onset of senescence (break-point of the chlorophyll concentration) at each leaf position (see gray arrows, Fig. 2) were consistent with that observed for GLAI: senescence started later, in all positions, in the leaves of the SG hybrid.

3.5. Net photosynthesis

The dynamics of net photosynthesis in all four targeted leaf positions, and the differences in these dynamics between hybrids and leaf positions, are exemplified for Year 1 in Fig. 4. The main features of Pn responses to hybrid, leaf position, and thermal time from achievement of maximum leaf expansion were similar to those exhibited by leaf chlorophyll levels. The maximum (plateau) values of Pn were statistically indistinguishable between hybrids and leaf positions. In leaves at all four positions, the falling phase began significantly ($p < 0.05$) later in the SG hybrid, and in Leaves 20, 22 and 24 –but not in Leaf 17- the leaves of the SG hybrid exhibited higher rates of Pn throughout the duration of the falling period. Small, and in some cases significant, variations between leaf positions in the timing of the start of the falling phase or between hybrids and leaf positions in the slope of the falling phase did not alter this general picture. Much of the interaction between leaf positions (Tables S2 and S3, Supplementary material) for Pn was due to the differences in temporal pattern between Leaf 17 and leaves of the remaining three positions. Importantly, the start of the falling phase in Pn was clearly associated with the timing of the fall in chlorophyll (see broad arrows, Fig. 4).

3.6. PSII quantum yield

The dynamics of *Fv/Fm* in all four targeted leaf positions, and the differences in these dynamics between hybrids and leaf positions, are exemplified for Year 1 in Fig. 5. As with chlorophyll and Pn, the broad picture was one of a lack of differences among leaf positions and hybrids for the maximum (plateau) values of *Fv/Fm*, a delay in the timing of the start of the falling phase in the SG hybrid which, combined with generally small differences in the slope of the falling phase, led to greater *Fv/Fm* values in leaves of the SG hybrid in all four positions including, in the case of this variable, Leaf 17. Small, albeit sometimes significant, differences in the timing of the start of the falling phase between leaf positions and in the slope of the falling phase between hybrids or leaf positions (Tables S2 and S3, Supplementary material) did not alter this picture in any important way. As with Pn, the timing of the start of the falling phase in *Fv/Fm* values across positions and hybrids was closely associated with the timing of the fall in leaf chlorophyll values (see broad arrows in Fig. 5).

3.7. Leaf trans-Zeatin levels

The dynamics of *trans*-Zeatin in all four targeted leaf positions and the differences in these dynamics between hybrids and leaf positions are exemplified for Year 1 in Fig. 6. Outstanding features of the *trans*-Zeatin dynamics were the very large and significant ($p < 0.05$) differences between hybrids and across all four positions of the initial (plateau) levels of *trans*-Zeatin, a significant ($p < 0.05$) delay in the timing of the start of the falling phase in the SG hybrid, and a significant ($p < 0.05$) difference in the slope of the falling phase (greater in the SG hybrid) (Tables S2 and S3, Supplementary material). The difference in initial *trans*-Zeatin values between SG and FDD hybrids was so great that the leaves of the former maintained greater values of *trans*-Zeatin during the whole measurement period. There were some significant interactions between hybrids and leaf position for the initial (plateau) values of *trans*-Zeatin (with a significant [$p < 0.05$] decrease with leaf position in FDD and generally significant [$p < 0.05$] increases in SG), in the timing of the start of the falling phase between leaf positions and for the slope of the falling phase, but these did not alter the general picture. As with Pn and *Fv/Fm*, there was a strong association −across leaf positions and hybrids- between the timings in the start of the fall of *trans*-Zeatin values and those of chlorophyll (see broad arrows in Fig. 6).

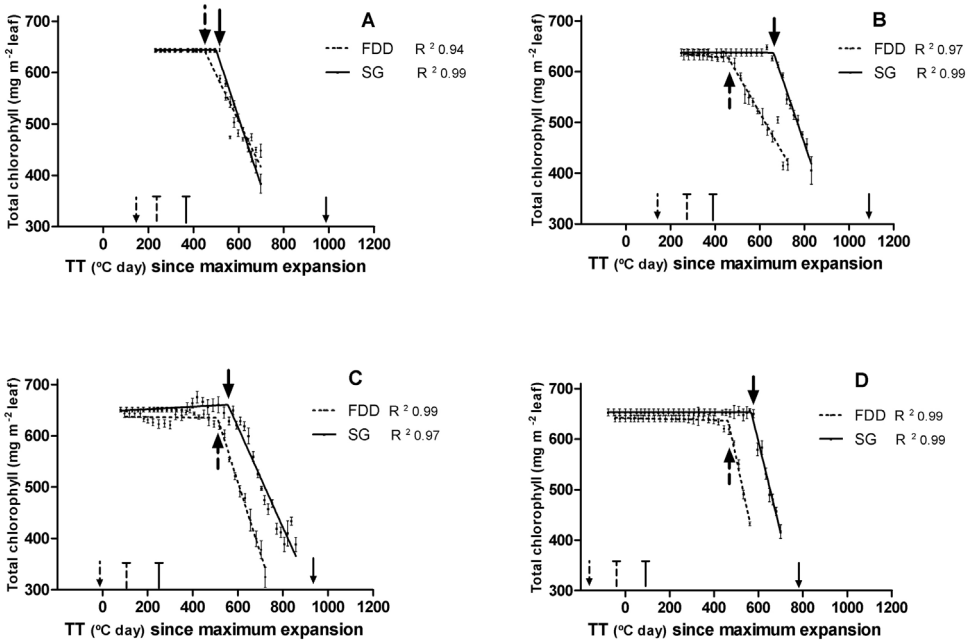

Fig. 3. Dynamics, during grain filling, of total chlorophyll content (mg m^{-2} leaf) for leaf positions 17 (A), 20 (B), 22 (C) and 24 (D) in SG and FDD hybrids as a function of thermal time (T_b = 4 °C) since achievement of maximum leaf expansion at each position. The onset time of the fall in chlorophyll levels is indicated with a full (SG) or dashed (FDD) broad arrows. The small narrow arrows close to "x" axis indicate the timings of R5.1 (dashed arrow) and of R9 (full arrow). Capped vertical lines close to the "x" axis indicate the start of the falls in LRLD (dashed, FDD; full, SG). Capped vertical bars on data points indicate ± one S.E (n = 5). R^2 values for the fitted functions are shown next to treatment codes. For parameter values of fitted functions, see Table S3 in Supplementary material. Data from Year 1.

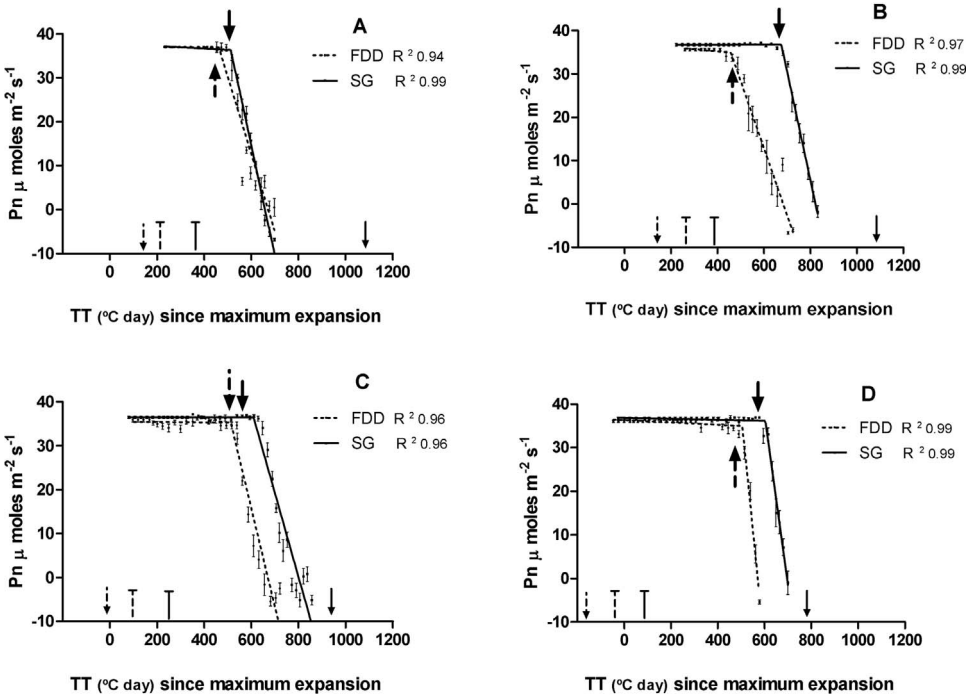

Fig. 4. Dynamics, during grain filling, of Net photosynthesis (Pn) (µ moles CO_2 m^{-2} s^{-1}) at a PPFD of 1500 µ moles m^{-2} s^{-1} for leaves in positions 17 (A), 20 (B), 22 (C) and 24 (D) in SG and FDD hybrids as a function of thermal time (T_b = 4 °C) since achievement of maximum leaf expansion at each position. The onset time of the fall in chlorophyll levels is indicated with full (SG), and dashed (FDD) broad arrows. The narrow arrows close to "x" axis indicates the timing of R5.1 (dashed arrow) and of R9 (full arrow). Capped vertical lines close to the "x" axis indicate the start of the falls in LRLD (dashed, FDD; full, SG). Capped vertical bars on data points indicate ± one S.E (n = 5). R^2 values for the fitted functions are shown next to treatment codes. For parameter values of fitted functions, see Table S3 in Supplementary material. Data from Year 1.

3.8. Comparative timing of changes (plateau > falling phase) in leaf variable dynamics

A comparison across leaf positions and hybrids of the timing of the change from plateau to falling phase for the set of four leaf variables considered (Table 1) showed that the timing of this shift was always significantly ($p < 0.05$) delayed in the SG hybrid with respect to the FDD hybrid. In addition, comparisons between leaf variables of the timing of this change within each leaf position for each hybrid showed the timings of the change in Pn and *trans*-Zeatin were statistically indistinguishable from those of chlorophyll in both hybrids, with the exception of leaf 24. By contrast, the timing of the change in *Fv/Fm* was

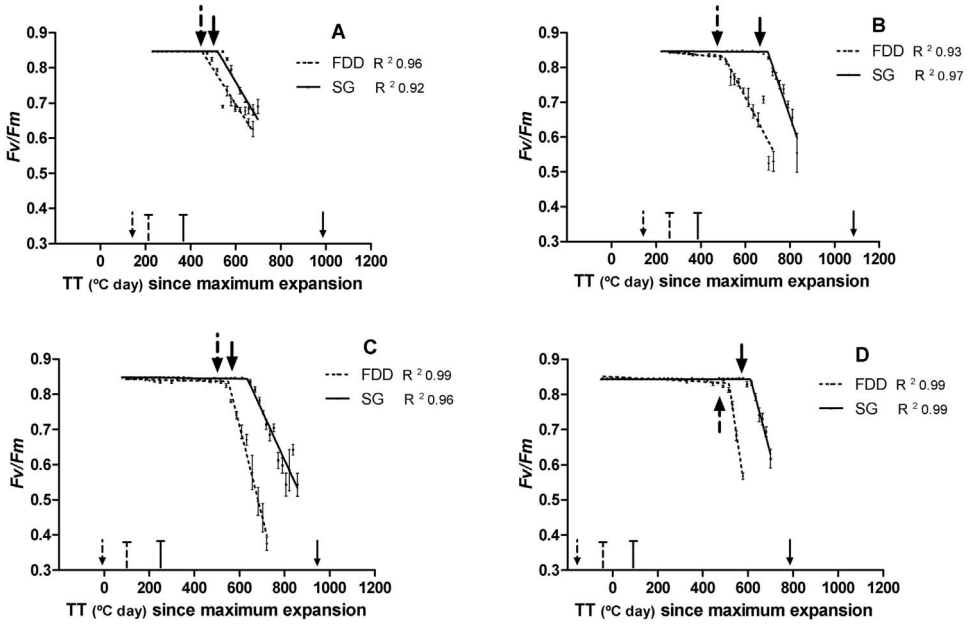

Fig. 5. Dynamics, during grain filling, of *Fv/Fm* for leaves in positions 17 (A), 20 (B), 22 (C) and 24 (D) in SG and FDD hybrids as a function of thermal time (T_b = 4 °C) since achievement of maximum leaf expansion at each position. The onset time of the fall in chlorophyll levels is indicated with a full (SG), and dashed (FDD) broad arrows. The narrow arrows close to "x" axis indicates the timing of R5.1 (dashed arrow) and of R9 (full arrow). Capped vertical lines close to the "x" axis indicate the start of the falls in LRLD (dashed, FDD; full, SG). Capped vertical bars on data points indicate ± one S.E (n = 5). R^2 values for the fitted functions are shown next to treatment codes. For parameter values of fitted functions, see Table S3 in Supplementary material. Data from Year 1.

slightly later than that of the other three variables in four out of eight hybrid by leaf position combinations. In our system, the timing of the shift from plateau to falling phase for chlorophyll proved a robust and simple to measure indicator of the start of leaf senescence, as reflected in the behavior of the other three leaf variables considered.

3.9. Responses to exogenous application of cytokinins

In both years, exogenous application of cytokinins (both BAP and *trans*-Zeatin) to Leaf 17 of both hybrids led to increases or maintenance, with a variable duration, of leaf *trans*-Zeatin levels or slowed the rate at which this variable fell with thermal time. Fig. 7 illustrates these responses for Year 1. The responses were greater in the FDD hybrid, as leaf *trans*-Zeatin values returned to or exceeded plateau values immediately after the first and second applications. In the SG hybrid there was some recovery in *trans*-Zeatin levels, but pre-application values were not achieved. In both hybrids, responses to a third application were very limited.

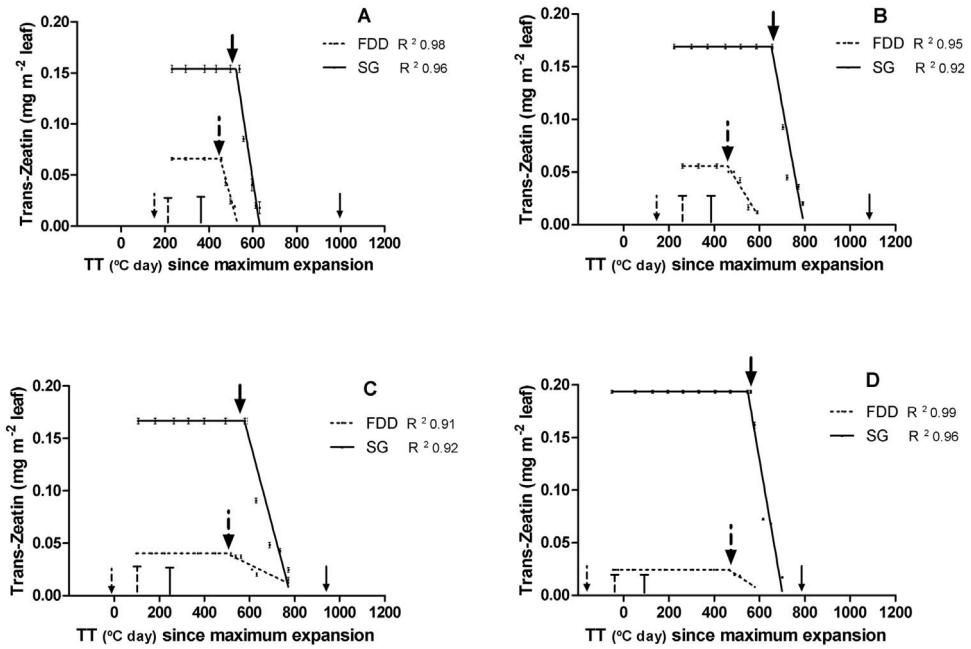

Fig. 6. Dynamics, during grain filling, of *trans*-Zeatin (mg m^{-2} leaf) for leaves in positions 17 (A), 20 (B), 22 (C) and 24 (D) in SG and FDD hybrids as a function of thermal time (T_b = 4 °C) since achievement of maximum leaf expansion at each position. The onset time of the fall in chlorophyll levels is indicated with full (SG), and dashed (FDD) broad arrows. The narrow arrows close to "x" axis indicates the timing of R5.1 (dashed arrow) and of R9 (full arrow). Capped vertical lines close to the "x" axis indicate the start of the falls in LRLD (dashed, FDD; full, SG). Capped vertical bars on data points indicate ± one S.E (n = 5). R^2 values for the fitted functions are shown next to treatment codes. For parameter values of fitted functions, see Table S3 in Supplementary material. Data from Year 1.

Table 1
Timing (in units of thermal time [T_b = 4 °C, Villalobos and Ritchie (1992)] after completion of leaf expansion) of change (plateau > falling phase) in leaf variable values (n = 5). Different lower case letters after each value indicate significant differences ($p < 0.05$) between timings of leaf variable changes within each hybrid x leaf position combination (row of table). Different upper-case letters after each value indicate significant differences ($p < 0.05$) between timings of leaf variable changes between hybrids for each leaf position. Data from Year 1.

Hybrid	*Leaf position*	*Total chlorophyll* TT (°Cday)			*Net photosynthesis* TT (°Cday)			*Fv/Fm* TT (°Cday)			*trans-Zeatin* TT (°Cday)		
FDD	*17*	449	a	B	462	a	B	451	a	B	451	a	B
SG	*17*	500	a	A	515	a	A	520	a	A	522	a	A
FDD	*20*	465	b	B	458	b	B	506	a	B	460	b	B
SG	*20*	660	a	A	676	a	A	702	a	A	653	a	A
FDD	*22*	508	b	B	512	b	B	551	a	B	499	b	B
SG	*22*	561	b	A	609	ab	A	633	a	A	577	ab	A
FDD	*24*	464	b	B	507	a	B	518	a	B	464	b	B
SG	*24*	567	bc	A	593	ab	A	612	a	A	547	c	A

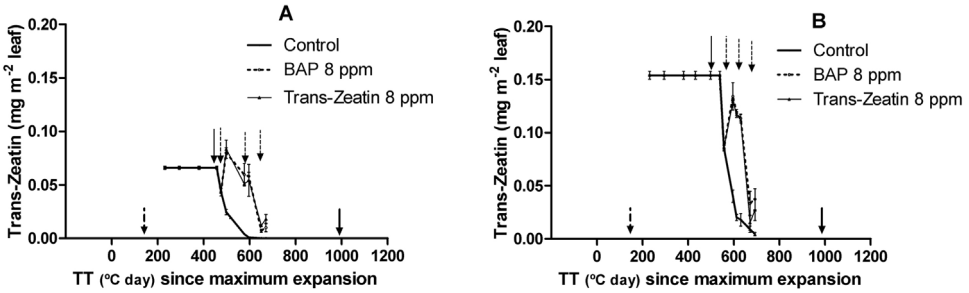

Fig. 7. Dynamics, during grain filling, of *trans*-Zeatin (mg m^{-2} leaf) for Leaf 17 in FDD (A) and SG (B) hybrids as a function of thermal time (T_b = 4 °C) since achievement of maximum leaf expansion at each position, in response to exogenous applications of 8 ppm BAP and *trans*-Zeatin solutions. The onset time of the fall in chlorophyll levels in the control treatment is indicated with a full arrow, and the moments of application with dashed arrows. The small arrows close to "x" axis indicates the timing of R5.1 (dashed arrow) and of R9 (full arrow). Capped vertical bars on data points indicate ± one S.E (n = 5). Data from Year 1.

The three applications of BAP and the first two applications of *trans*-Zeatin had the effect of maintaining chlorophyll values in both hybrids at values close to 90% of the plateau levels observed before the leaves began to senesce. The exception to this was the third application with *trans*-Zeatin in which the values were lower than the 90% mentioned (Fig. 8). In both hybrids, the first exogenous application of both forms of cytokinins also maintained the values of net photosynthesis and *Fv/Fm*, and with the second application the values of these variables returned close to pre-senescence plateau values (Fig. 8). By contrast, the third application had a much smaller impact. In this context, we estimated a threshold cytokinin value as from which the onset of leaf senescence occurs, in both types of cytokinins, as the average of *trans*-Zeatin values, between the first application and before the third application (for FDD from 473 °Cd to 598 °Cd, and for SG from 542 °Cd to 622 °Cd from maximum expansion) because it was the time interval during which the exogenous applications of both forms of cytokinins maintained chlorophyll levels, net photosynthesis and *Fv/Fm*. These two values per each hybrid were averaged. For FDD the threshold estimate was 0.06 mg m^{-2} leaf (equivalent to 245 ngg^{-1} fresh weight) and for SG it was 0.13 mg m^{-2} leaf (equivalent to 542 ng g^{-1} fresh weight). There were no significant ($p > 0.05$) differences between these threshold value estimates and the initial plateau values shown in Fig. 6 for leaves at position 17.

3.10. Intensity and quality of light incident on target leaves

The values of PAR and of R/FR of the light incident on leaves of the four positions, as measured at several times after the beginning of anthesis, are exemplified for Year 1 in Table 2. Across the 4 dates, PAR and R/FR tended to increase (sometimes significantly [$p < 0.05$]) with leaf position in both hybrids. In both variables, no significant ($p > 0.05$) differences were found, in each hybrid x leaf position combination, between times of measurement. While there were no significant differences between hybrids for each specific leaf position/date combination, values of both variables for SG were lower than for FDD, thus suggesting that PAR and R/FR were not the signals involved in determining differences between hybrids in the onset of leaf senescence.

4. Discussion

Differences between hybrids in canopy senescence could not be attributed to variations in crop development or in environmental conditions to which the hybrids were exposed (see Section 3.1). In addition, differences between hybrids were not associated with differences in PAR and/or light quality (R/FR ratio) impinging on target leaves (Table 2). These last results contrast with those of (Rousseaux et al., 1996, 2000) who found that, in the pre-anthesis phase, a reduction in PAR and/or R/FR ratio can initiate leaf senescence, suggesting that in the post-anthesis phase, during which the weight of the fruit is fixed, other controls operate.

Our data are consistent with those of Lisanti et al. (2013), insofar as in both hybrids (a different pair of SG and FDD hybrids to that used by Lisanti) LRLD began to fall before GLAI (Figs. 1 and 2). Our results deepen and broaden those of Lisanti et al. (2013). They found that live root length density began to decrease before leaf senescence during the grain filling phase became evident. Our results add to these findings because, as well as confirming that live root density begins to fall before leaf senescence is initiated, they also show that there is a direct association between the onset of the fall in foliar cytokinin levels and the onset of leaf senescence, as reflected in falls in leaf chlorophyll levels, in net photosynthesis and in *Fv/Fm*. Our results suggest that a plausible explanation for the control of the canopy senescence process and its differences between hybrids is a fall in root activity as a source of cytokinins leading to a fall in leaf cytokinin levels. Others, working with other species, such as tobacco (Singh et al., 1992; Gan and Amasino, 1995; Ori et al., 1999), lettuce (*Lactuca sativa* L.) (McCabe et al., 2001), *Phragmites australis* (Conrad et al., 2015), rice (Liu et al.,

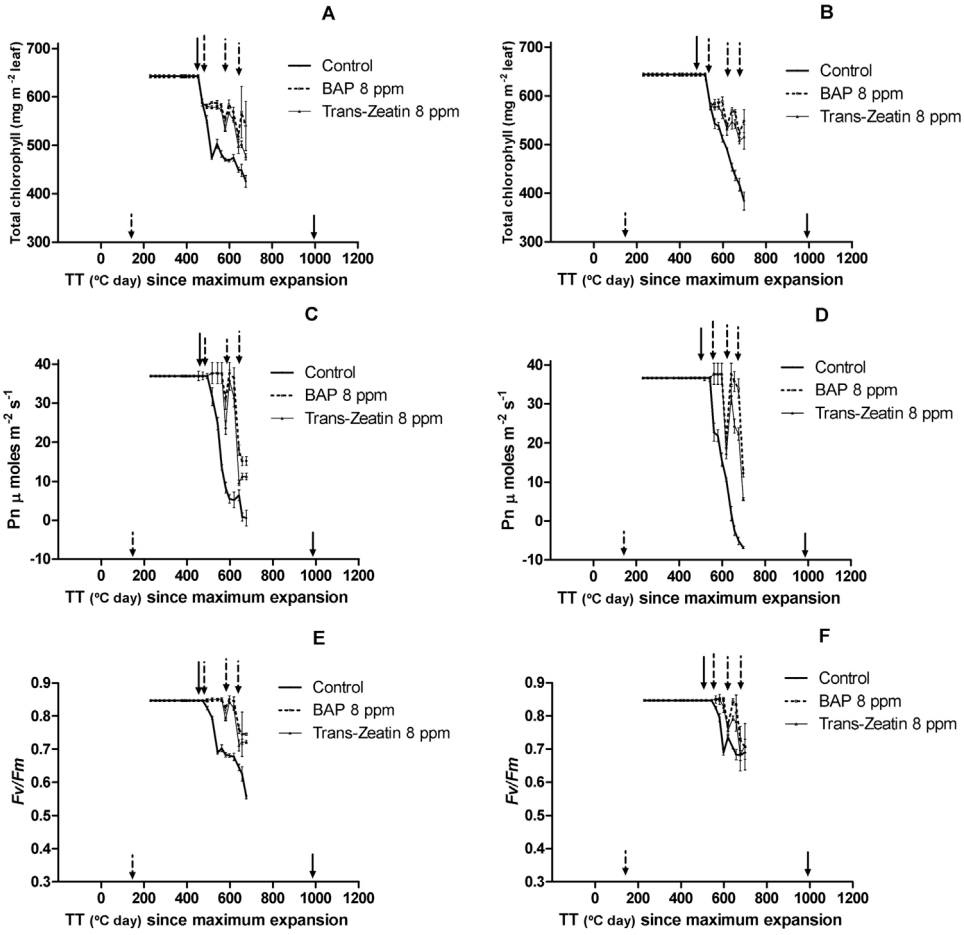

Fig. 8. Dynamics, during grain filling, of total chlorophyll content (mg m^{-2} leaf) (A, B), Net photosynthesis (Pn) (μ moles m^{-2} s^{-1}) (C, D) and *Fv/Fm* (E, F) for Leaf 17 in FDD (A, C, E) and SG (B, D, F) hybrids as a function of thermal time (T_b = 4 °C) since achievement of maximum leaf expansion at each position, in response to exogenous applications of 8 ppm solutions of BAP and of *trans*-Zeatin. The onset time of the fall in chlorophyll levels in the control treatment is indicated with a full arrow, and the moments of application with dashed arrows. The small arrows close to "x" axis indicates the timing of R5.1 (dashed arrow) and of R9 (full arrow). Capped vertical bars on data points indicate ± one S.E (n = 5). Data from Year 1.

2016), maize (Ren et al., 2016), Xanthium (Richmond and Lang, 1957), soybean (Noodén et al., 1979) and *Arabidopsis thaliana* L. (Masferrer et al., 2002), have shown that falls in leaf cytokinin levels are associated the start of leaf senescence, and in sorghum, Ambler et al. (1992) shown that the xylem sap cytokinin concentrations were higher in a delayed senescence genotype. None of the above reports have linked these effects to measures of root functionality.

Our results also show that total chlorophyll per unit of leaf area is a good indicator of the start of the decrease in the levels of other indicators of leaf functionality because in most cases no significant differences were found between the timing of initiation of the decreases in the levels of the four leaf variables analyzed (Table 1). For all measured leaf variables and in all leaf positions, values for FDD decreased before those of the SG hybrid (Figs. 2 [numbered grey arrows] and 3–6). The break-points in the bilinear functions fitted to leaf-level variables (Figs. 3–6) took place, as the level of insertion of the

Table 2
Values of PAR (μmol m^{-2} s^{-1}) and red/far-red ratio relationship (n = 5 for both variables), for four leaf positions of each hybrid measured at the beginning of R5 (1 DFBA), R6 (12 DFBA), R7 (22 DFBA), and R8 (30 DFBA). The timings of the onset of leaf senescence at specific positions were: FDD hybrid, leaf positions 17 (14 DFBA), 20 (18 DFBA), 22 (23 DFBA) and 24 (28 DFBA); SG hybrid, leaf positions 17 (17 DFBA), 20 (24 DFBA), 22 (27 DFBA) and 24 (35 DFBA). Within each variable, different letters after values within a column indicate significant differences ($p < 0.05$) between hybrids for each leaf position, at each time of observation; while different letters after values within a line indicate significant differences ($p < 0.05$) between the 4 times of observation, for each hybrid x leaf position combination. Data from Year 1.

Time of measurement (DFBA)		*1*		*12*		*22*		*30*		*1*		*12*		*22*		*30*	
		PAR radiation (μmol m^{-2} s^{-1})								*Red/Far red ratio*							
Incident outside the canopy		*1589*		*1514*		*1474*		*1363*		*1.10*		*1.11*		*1.12*		*1.08*	
Hybrid	*Leaf position*																
FDD	*17*	60	a	58	a	74	a	83	a	0.24	a	0.23	a	0.22	a	0.26	a
	20	265	cd	264	cd	269	d	281	d	0.56	b	0.55	b	0.55	b	0.6	b
	22	266	cd	264	cd	266	cd	283	d	0.60	b	0.58	b	0.59	b	0.62	b
	24	440	e	438	e	442	e	427	e	0.64	b	0.64	b	0.62	b	0.61	b
SG	*17*	38	a	36	a	36	a	58	a	0.20	a	0.19	a	0.17	a	0.22	a
	20	75	a	74	a	79	a	80	a	0.26	a	0.25	a	0.25	a	0.26	a
	22	208	b	205	b	210	b	221	bc	0.28	a	0.28	a	0.27	a	0.27	a
	24	313	d	311	d	309	d	302	d	0.66	b	0.65	b	0.68	b	0.68	b

leaf being considered increased, at increasing values of thermal time after the start in the fall in LRLD values. If, as our results suggest, the rate of supply of root-derived cytokinin to the leaves is an important factor in regulating leaf senescence, these differences between leaf positions indicate that differences in the partitioning of xylem flow between leaves may also play a role in determining the sequence of senescence with leaf position. Neumann and Stein (1984) have shown that a decrease in xylem sap flux to leaves precedes senescence. Possibly, differences in leaf exposure to incoming radiation (Table 2) and hence, leaf transpiration, may be involved. However, it should not be overlooked that leaf senescence is a complex process in which the effects of several internal and external signals are integrated into age-dependent senescence pathways (Lim et al., 2007), and that and interaction between root cytokinin supply, radiation and transpiration may not be the only control involved.

Our initial hypothesis that the differences between SG and FDD in leaf senescence dynamics was solely due to a difference in timing of the fall, from initially similar levels in both hybrids, of *trans*-Zeatin in leaves was shown to be inappropriate because of the large differences between hybrids in plateau values of *trans*-Zeatin (Fig. 6). Rather, the onset of senescence in leaves of both hybrids was associated with a very different *trans*-Zeatin threshold which marks the start of the fall-off. The *trans*-Zeatin threshold, in leaf 17 for FDD was 0.06 mg m^{-2} leaf [equivalent to 245 ngg^{-1} fresh weight] and for SG was 0.13 mg m^{-2} leaf [equivalent to 542 ngg^{-1} fresh weight]. If the lack of significant ($p > 0.05$) differences, in both hybrids, between the values of the threshold estimated from leaf responses to exogenous cytokinins and the steady-state (i.e., pre-decrease) levels of endogenous cytokinins in Leaf position 17 were to apply to the remaining leaf positions, it would suggest that the plateau values for these leaves could be taken as an estimate of the threshold value below which the leaf senescence process is initiated (falls in total chlorophyll and in photosynthetic process variables). This has not been observed before, in sunflower or in any other crop species, and suggests that simple comparisons of the *trans*-Zeatin concentration are not effective and that different between-hybrid sensitivities to *trans*-Zeatin levels need to be factored in before the full picture emerges. In addition, the higher levels of LRLD throughout the measurement period in the SG hybrid [Fig. 1] may have been a key factor to determine the differences between hybrids in the levels of *trans*-Zeatin in the leaves.

The responses to external applications of cytokinins are consistent with the notion of a linkage between the start of root senescence and the onset of leaf senescence, as high levels of cytokinins in the leaves (which correspond to high values of LRLD) cause a delay in leaf senescence, reflected in a later start in the fall of total chlorophyll and a slower rate of decrease (Fig. 8A and B) and in the recovery of photosynthesis (Fig. 8C and D) and *Fv/Fm* (Fig. 8E and F) values. These results strengthen the connection between root system functionality and leaf senescence, and may be due a possible decrease of the cytokinin content in the xylem fluid, or to the decrease in xylem sap flux to leaves (Neumann and Stein 1984) or a combination of both. This has not been reported before for sunflower hybrids of contrasting canopy senescence patterns. The differences between hybrids in the behavior of the endogenous levels of leaf cytokinin after exogenous applications (Fig. 7) may reflect a greater rate of degradation of cytokinins by the SG hybrid, or differences in the responses to cytokinin levels by the corresponding receptors, issues which merits further investigation.

In conclusion, our results show for the first time in sunflower crops and from experiments conducted under field conditions the fundamental role of the dynamics of cytokinin levels in the onset of leaf senescence in hybrids of contrasting canopy senescence patterns during grain-filling, high-lighting the connection between the start of the falling phase in leaf cytokinin levels and the start of leaf senescence in hybrids of very different plateau levels of cytokinins. In addition, these results emphasize the connections between the start of the fall of LRLD in the two hybrids, and the start of the falls in GLAI and leaf functionality variables.

The SG trait is known to influence crop functioning during grain-filling. Lisanti et al. (2013) have shown, under both drought and well-watered conditions, that a SG sunflower hybrid maintained greater soil water extraction rates for a longer time after flowering than a FDD hybrid, a behavior which has positive effects on grain yield (Lisanti, pers. comm.); and De la Vega et al. (2011) have shown that the SG hybrids accumulate greater biomass during grain-filling. Exogenous applications of cytokinins have been found to delay leaf senescence in both FDD and SG hybrids, generating increases in grain yield (Chimenti, pers. comm.). Our results advance current understanding, at both crop and leaf levels, of the controls and consequences of SG during grain filling, providing further evidence that breeding efforts aimed at profiting from this trait to increase crop yields are worthwhile.

Acknowledgments

We thank Nidera Semillas SAIC for access to seed of the hybrids used in the experiments. This research was supported by grants from UBACyT (UBA 20020100100017) and FONCyT (PICT 1765). Mariano Mangieri was in receipt, successively, of FONCyT and CONICET scholarships and AJH is a member of CONICET, the National Research Council of Argentina.

Appendix A. Supplementary data

Supplementary data associated with this article can be found, in the online version, at http://dx.doi.org/10.1016/j.eja.2017.03.007.

References

Akiyoshi, D.E., Morris, R.O., Hinz, R., Mischke, B.S., Kosuge, T., Garfinkel, D.J., Gordon, M.P., Nester, E.W., 1983. Cytokinin/auxin balance in crown gall tumors is regulated by specific loci in the T-DNA. Proc. Natl. Acad. Sci. U. S. A. 80, 407–411.
Akiyoshi, D.E., Klee, H., Amasino, R.M., Nester, E.W., Gordon, M.P., 1984. T-DNA of Agrobacterium tumefaciens encodes an enzyme of cytokinin biosynthesis. Proc. Natl. Acad. Sci. U. S. A. 81, 5994–5998.
Ambler, J.R., Morgan, P.W., Jordan, W.R., 1992. Amounts of zeatin and zeatin riboside in xylem sap of senescent and nonsenescent sorghum. Crop Sci. 32, 411–419.
Angadi, S.V., Entz, M.H., 2002. Root system and water use patterns of different height sunflower cultivars. Agron. J. 94, 136–145.
Barry, G.F., Rogers, S.G., Fraley, R.T., Brand, L., 1984. Identification of cloned cytokinin biosynthetic gene. Proc. Natl. Acad. Sci. U. S. A. 81, 4776–4780.
Beveridge, C.A., Murfet, I.C., Kerhoas, L., Sotta, B., Miginiac, E., Rameau, C., 1997. The shoot controls zeatin riboside export from pea roots. Evidence from the branching mutant rms4. Plant J. 11, 339–345.
Buchanan- Wollaston, V., Earl, S., Harrison, E., Mathas, E., Navabpour, S., Page, T., Pink, D., 2003. The molecular analysis of leaf senescence–a genomics approach. Plant Biotechnol. J. 1, 3–22.
Conrad, K., Motyka, V., Bernhardt, R., Stein, C., 2015. Cytokinin dynamics in differently senescing laminae of Phragmites australis plants grown in different habitats. S. Afr. J. Bot. 99, 54–61.
De la Vega, A.J., Cantore, M.A., Sposaro, M.M., Trápani, N., López Pereira, M., Hall, A.J., 2011. Canopy stay-green and yield in non-stressed sunflower. Field Crops Res. 121, 175–185.
Di Rienzo, J.A., Casanoves, F., Balzarini, M.G., Gonzalez, L., Tablada, M., Robledo, C.W., 2010. InfoStat Version 2010. InfoStat Group, Facultad de Ciencias Agrarias, Universidad Nacional de Córdoba, Argentina.
Dosio, G., Popovich, J., Lorenzo, M., Aguirrezabal, L., 2010. Cronología de eventos relacionados con la senescencia foliar en girasol. 5to. Congreso Argentino de girasol, ASAGIR, 1-2 de Junio 2010. Resumenes 5to. Congreso Argentino de Girasol. pp. 303.
Gan, S., Amasino, R.M., 1995. Inhibition of leaf senescence by autoregulated production of cytokinin. Science 270, 1986–1988.
Gan, S., Amasino, R.M., 1997. Making sense of senescence. Plant Physiol. 113, 313–319.
Gregersen, P.L., Holm, P.B., Krupinska, K., 2008. Leaf senescence and nutrient remobilization in barley and wheat. Plant Biol. 10, 37–49.
Gregory, P.J., McGowan, M., Biscoe, P.V., Hunter, B., 1978. Water relations of winter wheat. 1: growth of the root system. J. Agric. Sci. 91, 91–102.
Guiamét, J.J., Willemoes, J.G., Montaldi, E.R., 1989. Modulation of progressive leaf senescence by the red: far-red ratio of incident light. Botanical Gazette 150, 148–151.
Guiamét, J.J., Pichersky, E., Noodén, L.D., 1999. Mass exodus from senescing soybean chloroplasts. Plant Cell Physiol. 40, 986–992.
Guiboileau, A., Sormani, R., Meyer, C., Masclaux-Daubresse, C., 2010. Senescence and death of plant organs: nutrient recycling and developmental regulation. Comptes Rendus Biologies 333, 382–391.

He, Y., Tang, W., Swain, J.D., Green, A.L., Jack, T.P., Gan, S., 2001. Networking senescence-regulating pathways by using arabidopsis enhancer trap lines. Plant Phisiol. 126, 707–716.
Hoyerová, K., Gaudinová, A., Malbeck, J., Dobrev, P., Kocábek, T., Šolcová, B., Trávníčková, A., Kamínek, M., 2006. Efficiency of different methods of extraction and purification of cytokinins. Phytochemistry 67, 1151–1159.
Inskeep, W.P., Bloom, P.R., 1985. Extinction coefficients of chlorophyll *a* and *b* in *N,N*-Dimethylformamide and 80% acetone. Plant Physiol. 77, 483–485.
Itai, C., Vaadia, Y., 1971. Cytokinin activity in water-stressed shoots. Plant Physiol. 47, 87–90.
Lamattina, L., Pont Lezica, R., Conde, R.D., 1985. Protein metabolism in senescing wheat leaves: determination of synthesis and degradation rates and their effects on protein loss. Plant Physiol. 77, 587–590.
Lim, P.O., Kim, H.J., Nam, H.G., 2007. Leaf senescence. Ann. Rev. Plant Biol. 58, 115–136.
Lisanti, S., Hall, A.J., Chimenti, C.A., 2013. Influence of water deficit and canopy senescence pattern on Helianthus annuus (L.) root functionality during the grain-filling phases. Field Crops Res. 154, 1–11.
Liu, L., Li, H., Zeng, H., Cai, Q., Zhou, X., Yin, C., 2016. Exogenous jasmonic acid and cytokinin antagonistically regulate rice flag leaf senescence by mediating chlorophyll degradation, membrane deterioration, and senescence-associated genes expression. J. Plant Growth Regul. 35, 366–376.
Martínez, D.E., Costa, M.L., Gomez, F.M., Otegui, M.S., Guiamét, J.J., 2008. Senescence-associated vacuoles are involved in the degradation of chloroplast proteins in tobacco leaves. Plant J. 56, 196–206.
Masferrer, A., Arró, M., Manzano, D., Schaller, H., Fernández-Busquets, X., Monceleán, P., Fernández, B., Cunillera, N., Boronat Ferrer, A., 2002. Overexpression of Arabidopsis thaliana farnesyl diphosphate synthase (FPS1S) in transgenic Arabidopsis induces a cell death/senescence-like response and reduced cytokinin levels. Plant J. 30, 123–132.
McCabe, M.S., Garratt, L.C., Schepers, F., Jordi, W.J.R.M., Stoopen, G.M., Davelaar, E., Van Rhijn, H.A., Power, J.B., Davey, M.R., 2001. Effects of PSAG12-IPT gene expression on development and senescence in transgenic lettuce. Plant Physiol. 127, 505–516.
Mengel, D.B., Barber, S.A., 1974. Development and distribution of the corn root system under field conditions. Agron. J. 66, 341–344.
Neumann, P.M., Stein, Z., 1984. Relative rates of delivery of xylem solute to shoot tissues: possible relationship to sequential leaf senescence. Physiol. Plant. 62, 390–397.
Noodén, L.D., Kahanak, G.M., Okatan, Y., 1979. Prevention of monocarpic senescence in soybeans with auxin and cytokinin: an antidote to self-destruction. Science 206, 841–843.
Noodén, L.D., Singh, S., Letham, S., 1990. Correlation of xylem sap cytokinin levels with monocarpic senescence in soybean. Plant Physiol. 93, 33–39.
Noodén, L.D., Guiamét, J.J., John, I., 1997. Senescence mechanisms. Physiol. Plant. 101, 746–753.
Ori, N., Juarez, M.T., Jackson, D., Yamaguchi, J., Banowetz, G.M., Hake, S., 1999. Leaf senescence is delayed in tobacco plants expressing the maize homeobox gene knotted1 under the control of a senescence-activated promoter. Plant Cell 11, 1073–1080.
Pereyra, V.R., Farizo, C., Cardinali, F., 1982. Estimation of leaf area on sunflowerplants. In: Proc. 10th Int. Sunflower Conf. Surfers Paradise, Australia. March 14–18, 1982, International Sunflower Association, Paris. pp. 21–23.
Pic, E., de la Serve, B.T., Tardieu, F., Tur, O., 2002. Leaf senescence induced by mild wáter déficit follows the same sequence of macroscopic, biochemical, and molecular events as monocarpic senescence in Pea. Plant Physiol. 128, 236–246.
Rajcan, I., Tollenaar, M., 1999. Source: sink ratio and leaf senescence in maize: I. Dry matter accumulation and partitioning during grain filling. Field Crops Res. 60, 245–253.
Rajcan, I., Dwyer, L.M., Tollenaar, M., 1999. Note on relationship between leaf soluble carbohydrate and chlorophyll concentrations in maize during leaf senescence. Field Crops Res. 63, 13–17.
Ren, B., Zhu, Y., Zhang, J., Dong, S., Liu, P., Zhao, B., 2016. Effects of spraying exogenous hormone 6-benzyladenine (6-BA) after waterlogging on grain yield and growth of summer maize. Field Crops Res. 188, 96–104.
Richmond, A.E., Lang, A., 1957. Effect of kinetin on protein content and survival of detached Xanthium leaves. Science 125, 650–651.
Rousseaux, M.C., Hall, A.J., Sánchez, R.A., 1996. Far-red enrichment and photosynthetically active radiation level influence leaf senescence in field-grown sunflower. Physiol. Plant. 96, 217–224.
Rousseaux, M.C., Hall, A.J., Sánchez, R.A., 2000. Basal leaf senescence in a sunflower (helianthus annuus) canopy: responses to increased R/RF ratio. Physiol. Plant. 110, 477–482.
Sadras, V.O., Hall, A.J., Trapani, N., Vilella, F., 1989. Dynamics of rooting and root-length: leaf-area relationships as affected by plant population in sunflower crops. Field Crops Res. 22, 45–57.
Sakakibara, H., 2006. Cytokinins: activity, biosynthesis, and translocation. Annu. Rev. Plant Biol. 57, 431–449.
Samuelson, M.E., Eliasson, L., Larsson, C.M., 1992. Nitrate-regulated growth and cytokinin responses in seminal roots of barley. Plant Physiol. 98, 309–315.
Schneiter, A.A., Miller, J.F., 1981. Description of sunflower growth stages. Crop Sci. 21, 901–903.
Sinclair, T.R., De Wit, C.T., 1976. Analysis of the carbon and nitrogen limitations to soybean yield. Agron. J. 68, 319–324.
Sinclair, T.R., Horie, T., 1989. Leaf nitrogen, photosynthesis, and crop radiation use efficiency: a review. Crops Sci. 29, 90–98.
Singh, S., Letham, D.S., Palni, L.M.S., 1992. Cytokinin biochemistry in relation to leaf senescence: VII. Endogenous cytokinin levels and exogenous applications of cytokinins in relation to sequential leaf senescence of tobacco. Physiol. Plant. 86, 388–397.
Sturite, L., Henriksen, T.M., Breland, T.A., 2005. Distinguishing between metabolically active and inactive roots by combined staining with 2,3,5-triphenyltetrazolium chloride and image colour analysis. Plant Soil 271, 75–82.
Takei, K., Sakakibara, H., Taniguchi, M., Sugiyama, T., 2001. Nitrogen-dependent accumulation of cytokinins in roots and the translocation to leaf: implication of cytokinin species that induces gene expression of maize response regulator. Plant Cell Physiol. 42, 85–93.
Van Oosterom, E.J., Chapman, S.C., Borrell, A.K., Broad, I.J., Hammer, G.L., 2010. Functional dynamics of the nitrogen balance of sorghum: II. Grain filling period. Field Crops Res. 115, 29–38.
Villalobos, F.J., Ritchie, J.T., 1992. The effect of temperature on leaf emergence rates of sunflower genotypes. Field Crops Res. 29, 37–46.
White, P.R., 1934. Potentially unlimited growth of excised tomato root tips in a liquid medium. Plant Physiol. 9, 585–600.